Journal of Traditional and Complementary Medicine 14 (2024) 675–686

Contents lists available at ScienceDirect

Journal of Traditional and Complementary Medicine

journal homepage: www.elsevier.com/locate/jtcme

Integrated skin metabolomics and network pharmacology to explore the mechanisms of Goupi Plaster for treating knee osteoarthritis

Jia Liu [a,1], Yingpeng Li [b,1], Jiajing Wang [c], Bixi Guan [a], Zhaoliang Chen [a], Ziheng Liu [a], Yunfeng Xue [a], Yongji Li [a], Feng Guan [a], Yanhong Wang [a,*]

[a] Key Laboratory of Basic and Application Research of Beiyao, Heilongjiang University of Chinese, Harbin, 150040, China
[b] College of Chinese Medicine, Tianjin University of Traditional Chinese Medicine, Tianjin, 300193, China
[c] Heilongjiang University of Chinese Medicine Affiliated Second Hospital, Harbin, China

ARTICLE INFO

Keywords:
Goupi Plaster (GP)
Knee osteoarthritis
Mechanisms
Metabonomics
Network pharmacology

ABSTRACT

Background and aim: Goupi Plaster (GP) is topical traditional Chinese medicine preparation. It has been used to treat Knee Osteoarthritis (KOA) in clinical practice of traditional Chinese medicine (TCM). However, the mechanisms of GP relieve KOA are poorly understood.

Experimental procedure: Rabbit models of KOA were established and treated with GP. Knee cartilage pathology was analyzed using hematoxylin and eosin staining, while plasma levels of inflammatory factors (interleukin (IL)-4, IL-6, and IL-17) and skin neurotransmitters (calcitonin gene-related peptide (CGRP), substance P (SP), and5-hydroxytryptamine (5-HT)) were measured by enzyme linked immunosorbent assay. Metabolomics based on GC-TOF-MS analysis screened for skin biomarkers as well as relevant pathways. Network pharmacology screened for relevant skin targets as well as relevant pathways, and finally, MetScape software was utilized to integrate the results of metabolomics and network pharmacology to screen for key skin targets, key metabolites, and key pathways for GP treatment of KOA.

Results and conclusion: GP administration substantially repaired cartilage surface breaks in KOA and led to relatively intact cartilage structure and normal cell morphology. GP decreased plasma levels of IL-6 and IL-17 and skin levels of CGRP, SP and 5-HT while increased plasma IL-4. GP administration normalized the levels of 15 metabolites which were changed in KOA. Network pharmacology analysis identified 181 targets. Finally, 3 key targets, 5 key metabolites and 3 related pathways were identified, which suggested that GP improved skin barrier function and skin permeability by regulating skin lipid metabolism. GP treatment also regulated skin amino acid levels and subsequently affected neurotransmitters and signaling molecules. In addition, the purinergic signaling pathway was also involved in the treatment of GP against KOA.

In conclusion, GP treatment is associated with changes in skin lipid metabolism, neurotransmitters, and the purinergic signaling pathway.

1. Introduction

Knee osteoarthritis (KOA) is a degenerative disease that is characterized by articular cartilage degeneration, intra-articular and synovial inflammation, as well as lesions in subchondral and periarticular bones.[1] The disease is associated with aging, trauma, obesity, and genetics factors. A study in China between 2012 and 2016 found that 14.6 % of people had KOA, with 19.1 % of women and 10.9 % of men affected. The prevalence of KOA increases with age.[2] For comparison, in the United States, the prevalence of KOA is 33.6 %, with 42.1 % of women and 31.2 % of men affected. Similar to China, KOA prevalence in the US also increases with age and weight.[1] Data from the Chingford study in the United Kingdom showed that the prevalence of KOA was 17.6 % in women between the ages of 45 and 64.[3] In KOA pathogenesis,

Abbreviations: Goupi Plaster, GP; quality control, QC.

Peer review under responsibility of The Center for Food and Biomolecules, National Taiwan University.

* Corresponding author.
E-mail address: wangyanhong@hljucm.net (Y. Wang).

[1] Co-first author. Jia Liu and Yingpeng Li contributed equally.

https://doi.org/10.1016/j.jtcme.2024.04.004
Received 20 September 2023; Received in revised form 8 March 2024; Accepted 9 April 2024
Available online 12 April 2024

extracellular matrix degradation in the articular cartilage predisposes to cartilage erosion and fibrosis. Cartilage erosion results in release of proteoglycan and collagen fragments into the synovial fluid, leading to synovial inflammation and further articular cartilage degradation. Currently, non-steroidal anti-inflammatory drugs (NSAIDs) and glucocorticoids are commonly used to treat early-stage KOA. However, long-term use of these medications can result in severe adverse effects. Late-stage KOA requires joint replacement surgery which is expensive and is associated with post-operative complications.

Goupi Plaster (GP) is a classic Black Plaster that is prepared by heating vegetable oils containing active ingredients from herbs with lead oxide at high temperatures. It is composed of 29 medicinal materials[4] from Table 1, which contain many active ingredients that can treat KOA.[5] The active ingredient of *Cnidium monnieri* Cusson, osthole, has been reported to improve cartilage degradation by inhibiting the NF-κB and HIF-2α pathways in a mouse model of osteoarthritis.[6] *Sinomenium diversifolium* Diels is commonly applied in the treatment of rheumatoid arthritis (RA), osteoarthritis (OA) and gouty arthritis (GA).[7] Studies have shown that its active ingredient Sinomenine can suppress IL-1β-induced inflammatory response and cartilage destruction by activating the Nrf2/HO-1 signaling pathway and inhibiting the NF-κB signaling pathway.[8] Cinnamaldehyde, the active ingredient of *Cinnamomum cassia* (L.) J.Presl, confer protection on cartilage by modulating the miR-1285-5p/IL-20 axis and miR-140-5p/HMGB1/nuclear factor-κB pathway. They are commonly used in traditional medicine and play major therapeutic roles. For instance, herbs such as *Cinnamomum cassia* (L.) J. Presl and *Dipsacus asper* Wall. ex DC. can clear blocked pathways in the body, promote blood circulation, relieve pain,[9,10] and are utilized to treat bone paralysis, also known as OA.[11] All the above plant names have been checked with The World Flora Online (http://www.worldfloraonline.org). GP originated in the Jin Dynasty and was first recorded in "The Handbook of Prescriptions for Emergencies".[12] Traditionally, it was used for treating arthralgia caused by wind-cold damp pathogens and stagnation of blood.[4] Studies have shown that the topical application of GP can improved blood flow of the peri-knee arterial network in patients with KOA.[13] A clinical trial has shown that the combination of GP topical applications and quadriceps endurance training is more effective in treating KOA than intra-articular injections of sodium citrate alone.[14]

Table 1
The compositions of Goupi Plaster.

NO.	Chinese name	Latin name	Processing
1	Chuanwu	*Aconitum carmichaelii* Debeaux	Vegetable oils-Processed
2	Caowu	*Aconitum kusnezoffii* Rchb.	Vegetable oils-Processed
3	Qianghuo	*Notopterygium incisum* Ting ex H. T. Chang	Vegetable oils-Processed
4	Duhuo	*Angelica pubescens f. biserrata* R.H. Shan & C.Q.Yuan	Vegetable oils-Processed
5	Qingfengteng	*Sinomenium diversifolium* Diels	Vegetable oils-Processed
6	Xiangjiapi	*Periploca sepium* Bunge	Vegetable oils-Processed
7	Fangfeng	*Saposhnikovia divaricata* (Turcz.) Schischk.	Vegetable oils-Processed
8	Weilingxian	*Clematis chinensis* Osbeck	Vegetable oils-Processed
9	Cangzhu	*Atractylodes lancea* DC.	Vegetable oils-Processed
10	Shechuangzi	*Cnidium monnieri* Cusson	Vegetable oils-Processed
11	Mahuang	*Ephedra sinica* Stapf	Vegetable oils-Processed
12	Gaoliangjiang	*Alpinia officinarum* Hance	Vegetable oils-Processed
13	Xiaohuixiang	*Foeniculum vulgare* Mill.	Vegetable oils-Processed
14	Guangui	*Cinnamomum cassia* (L.) J.Presl	Vegetable oils-Processed
15	Danggui	*Angelica sinensis* (Oliv.) Diels	Vegetable oils-Processed
16	Chishao	*Paeonia lactiflora* Pall.	Vegetable oils-Processed
17	Mugua	*Chaenomeles speciosa* (Sweet) Nakai	Vegetable oils-Processed
18	Sumu	*Biancaea sappan* (L.) Tod.	Vegetable oils-Processed
19	Dahuang	*Rheum palmatum* L.	Vegetable oils-Processed
20	Yousongjie	*Pinus massoniana* Lamb.	Vegetable oils-Processed
21	Xuduan	*Dipsacus asper* Wall. ex DC.	Vegetable oils-Processed
22	Chuanxiong	*Ligusticum striatum* DC.	Vegetable oils-Processed
23	Baizhi	*Angelica dahurica* (Fisch.ex Hoffm.) Benth.et Hook.f.	Vegetable oils-Processed
24	Ruxiang	*Boswellia carteri* Birdw.	Powdered
25	Moyao	*Commiphora myrrha* Engl.	Powdered
26	Tianranbingpian	*Cinnamomum camphora* (L.) J.Presl	Powdered
27	Zhangnao	Camphor	Powdered
28	Dingxiang	*Eugenia caryophyllata* Thunb	Powdered
29	Rougui	*Cinnamomum cassia* (L.) J.Presl	Powdered

However, the mechanisms by which topical applications of GP relieves KOA are poorly understood. Generally, after topical application, the active ingredients of GP will penetrate into the subcutaneous tissue[15] to exert local effects and are absorbed into the blood and lymphatic vessels to exert systemic effects. Topical drugs indirectly relieve diseases by altering tissue as well as organ functions and regulating immune functions.[16] This indirect mechanism may be attributed to point stimulation and meridian transmission in TCM theory. The indirect therapeutic effects of topical applications of GP on KOA may be associated with neurotransmitter-mediated skin reactions. In this case, GP activates their respective receptors on the skin to ellicit distant effects at the knee joint via neurohormonal mediators. This exerts a broad therapeutic effect and can be a potential mechanism of action of topical preparations. To test this hypothesis, we investigated the therapeutic mechanism of GP on KOA through the skin by combining histopathological, biochemical, skin metabolomics and network pharmacological analyses.

The traditional experimental approaches for analyzing the synergistic mechanisms of multiple compounds, targets, and pathways are associated with various limitations. Metabolomics and network pharmacology are effective tools for elucidating the potential mechanisms of Chinese medicines.[17,18] Histopathologic analysis was performed to verify the therapeutic efficacy of GP. Plasma inflammatory factors (IL-4, IL-6, and IL-17) and skin neurotransmitters (CGRP, SP, and 5-HT) were measured to determine whether GP can treat KOA by modulating the neurotransmission pathways of the skin. IL-4 is a type 2 inflammatory factor that promotes tissue healing, promotes an immunomodulatory microenvironment in which joint-resident macrophages are polarized toward the M2 phenotype and efficiently scavenge pro-inflammatory debris, while osteoclasts maintain balanced levels of activity in the subchondral bone.[19] IL-6 is a pro-inflammatory cytokine which acts through a catabolic mechanism to upregulate the expression of MMP-1, MMP-13 and IL-1β in cartilage.[20] IL-17 accelerates the degradation of articular cartilage by stimulating the expression of inflammatory factors such as 1L-6,1L-8.[21] SP, CGRP, and 5-HT are involved in nociceptive signaling, play important roles in peripheral signaling and induction of nociceptive sensitization, and mediate neurogenic inflammatory responses.[22] In previous studies, it was found that application of moxibustion and acupuncture inhibited chondrocyte necrosis and alleviated pain in KOA mice by down-regulating the expression levels of SP and CGRP. They also altered the content of 5-HT, modified the microenvironment, and activated neural actions in the skin.[23] Metabolomics was performed to compare the changes in skin metabolites before and after GP treatment after which network pharmacology was developed to identify the relevant skin targets. Finally, the network pharmacology results were combined with metabolomics results to identify the key

targets, key metabolites and related pathways to explore the mechanisms of GP in KOA. The flow chart for this study is shown in Fig. 1.

2. Materials and methods

2.1. Reagents and instruments

The components of GP (Guizhou Jirentang Pharmaceutical Co., Ltd. Batch Number: 20180228) are presented in Table 1. Double-distilled H_2O was prepared using a Ming Che D 24 UV water-purification system from Merck Millipore (Germany). Papain was obtained from Sigma-Aldrich (USA, batch number: P3250). Methanol was obtained from CNW Technologies GmbH (Germany, grade: for HPLC). Chloroform and pyridine were provided by Adamas (Switzerland). Methoxymonium salt was obtained from Tokyo Chemical Industry Co., Ltd. (Japan, grade: for AR). Adonitol was procured from Sigma-Aldrich (USA, purity: 99 %). BSTFA was purchased from Regis Technologies, Inc (USA, with 1 % TMCS, v/v). FAMEs was obtained from Dr. Ehrenstorfer (Germany).

2.2. Experimental animals and treatment protocols

Healthy 20–24 weeks old male New Zealand rabbits (weighing 2.5 ± 0.2 kg) were obtained from Laboratory Animal Center of Heilongjiang University of Traditional Chinese Medicine (Harbin, China). The Animal Care and Ethics Committee at Heilongjiang University of Chinese Medicine approved this study (approval number: 2018102301; date: 20181023). The study was performed in accordance with the NIH Guidelines for Care and Use of Laboratory Animals (USA). All rabbits were housed in a temperature-controlled environment (25 ± 2 °C) with relative humidity of 55 ± 5 % and 12/12 h light/dark cycle and were given standard laboratory food and water ad libitum. Standard laboratory food was purchased from Liaoning Changsheng biotechnology co., Ltd. (China). They were allowed to acclamatize to the laboratory one week before the experiments.

They were randomized into three groups each with 8 rabbits: normal rabbits (control group, CON), KOA rabbits (model group, MOD) and GP-treated rabbits (GP- treated group, GP). The KOA rabbit models were established using the antigen induction method combined with ice-water bath stimulation. On days 1, 4, and 7, 0.5 mL of papain was injected into the intercondylar fossa of the hind limbs of the MOD and GP groups, and the rabbits were assisted to flex and extend their knee joints to facilitate proper diffusion of the induction agent. Next, their hind limbs were immersed in an ice-water mixture at −4 °C for 30 min every day for 7 consecutive days. On day 8, GP that had been heated and softened on a heating plate at 4 °C was applied to the knee joints of mice. Each GP was used for 60 h, and after removal, a new GP was applied 12 h later. This treatment was continued for 15 days.[13]

2.3. Sample collection

New Zealand white rabbits were anesthetized by injection of 1 % pentobarbital 20 mg/kg. After successful anesthesia, they were put on supine position on the operating table, and the neck was shaved and disinfected. An incision of approximately 2 cm in length was made in the middle of the neck, and the skin and subcutaneous tissues were incised to expose the trachea and to divest one side of the carotid artery, which was ligated distally and pierced proximally for blood.[24] Blood samples were centrifuged at 3000 rpm for 20 min to collect the supernatants.

Rabbits were sacrificed by air embolism to obtain the knee joint skin tissues, which were quenched using liquid nitrogen, and sliced into two parts.[25] One part was stored at −80 °C for subsequent analyses while the other parts were pulverized using a tissue grinder to remove the sediments to obtain knee joint skin tissue homogenates.[23]

Skin tissues from the knee joints were collected, and the medial malleolus joints of the femur were peeled off. The upper and lower 1 cm bone tissues were then separated and removed.[26]

2.4. Histopathological observation

The bone tissue was fixed with 4 % polydialdehyde and then decalcified with 10 % ethylenediamine. It was then embeddedin paraffin and sectioned. Finally, they were stained with H&E and the morphology was observed under an optical microscope.[26]

2.5. Biochemical analysis

The serum levels of inflammatory factors (IL-4, IL-6, and IL-17) and levels of skin tissue neurotransmitters (CGRP, SP, and 5-HT) in rabbits from each group were measured using ELISA kits following the manufacturer's instructions.[26] All kits were purchased from Nanjing Jiancheng Trading Co., Ltd. (China). The entire experiment was performed in accordance with the instructions on the kit.

Data from each group were imported into the Correlation Plot (Cytoscape 3.9.1 plug-in) for correlation analyses of plasma inflammatory factors and neurotransmitter levels in skin tissues.[27]

2.6. Skin metabolomics analyses

2.6.1. Sample pre-processing

The 50 mg refrigerated skin tissue samples placed in EP tubes that were supplemented with 1000 μL and 10 μL of the pre-cold extraction mixture (methanol/chloroform (v:v) = 3:1) and internal standard (adonitol, 0.5 mg/mL stock), respectively.

Samples were vortexed for 30 s, homogenized for 4 min, sonicated for 5 min in ice water and centrifuged at 10000 rpm and 4 °C for 15 min.

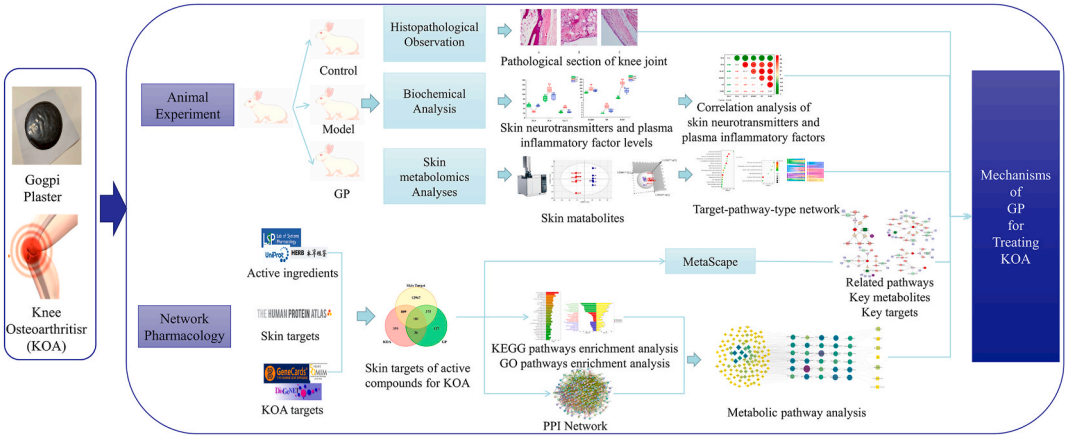

Fig. 1. The comprehensive strategy based on skin metabolomics and network pharmacology to explore the mechanisms of GP in KOA treatment.

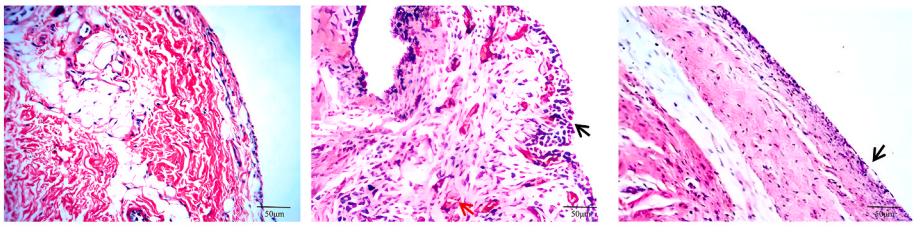

Fig. 2. H&E stained knee joint sections of different groups (× 200): (A) CON group (B) MOD group (C) GP group. Black arrows indicate cartilage surface destruction and red arrows indicate inflammation.

Then, 300 μL of the supernatants were transferred to a 1.5 mL tube to prepare the quality control (QC) samples. Fifty μL of each sample was removed and pooled.

Pooled samples were evaporated in a vacuum concentrator, supplemented with 30 μL methoxyamination hydrochloride and incubated at 80 °C for 30 min. Then, the samples were derivatized with 40 μL BSTFA regent at 70 °C for 1.5 h, gradually cooled to room temperature and supplemented with 5 μL FAMEs. Finally, all samples were analyzed by GC-TOF-MS.[25]

2.6.2. GC-TOF-MS analysis

A 7890 gas chromatograph (Agilent, USA) coupled with a time-of-flight mass spectrometer (LECO, USA) was used for analyses. It had a DB-5MS capillary column (Agilent, USA) that was injected with a splitless 1 μL aliquot of samples. Helium was used as the carrier gas, with a front inlet purge flow of 3 mL min^{-1}, and a flow rate of 1 mL min^{-1} through the column. The temperature was initially set to 50 °C for 1 min, increased to 310 °C at a rate of 10 °C min^{-1} and maintained at 310 °C for 8 min. The injection, transfer line, and ion source temperatures were 280 °C, 280 °C, and 250 °C, respectively. The energy used in electron impact mode was −70 eV. Mass spectrometry data were collected in full-scan modes with an m/z range of 50–500 at a rate of 12.5 spectra per second after solvent delay for 6.25 min.[25]

2.6.3. Data processing and analysis

Analysis on raw data, including peak extraction, baseline adjustment, deconvolution, alignment, and integration were performed using the Chroma TOF (V 4.3x, LECO, USA) software. Metabolite identification was performed using the LECO-Fiehn Rtx5 database matched mass spectra and retention indices.[28] Peaks that were found in less than half of the QC samples or in QC samples with RSD >30 % were removed.[29]

Processed data were imported into the SIMCA software (v14.1, Umetrics AB, Umea, Sweden) for multidimensional statistical analysis, including partial least squares discriminant analysis (PLS-DA) and orthogonal partial least squares discriminant analysis (OPLS-DA).[30] Differentially expressed metabolites between the MOD and GP groups were identified based on VIP values (VIP >1) and T-test ($p < 0.05$).[31,32] The biomarkers of KOA skin tissue among the differentially expressed metabolites were identified by performing T-tests ($p < 0.05$) on findings from the CON and MOD groups. Finally, the Human Metabolome Database[33] (HMDB, http://www.hmdb.ca/) and the Kyoto Encyclopedia of Genes and Genomes[34] (KEGG, http://www.genome.jp/kegg/) database were consulted to identify the potential roles of the metabolites. The MetaboAnalyst 4.0[35] (http://www.metaboanalyst.ca/) platform was used for pathway analysis. Parameters with an impact value > 0.1 as the index were used to identify the most relevant pathways.

2.7. Network pharmacology analysis

Active ingredients of GP in 29 Chinese herbal medicines were identified using drug-likeness (DL) ≥0.18[36] in the Traditional Chinese Medicine Systems Pharmacology Database and Analysis Platform[37] (TCMSP, https://old.tcmsp-e.com/tcmsp.php) and the HERB[38] (http://herb.ac.cn/) database. Even though the DL values were low, ingredients with clear pharmacological effects were selected for further studies. Information on targets of the active ingredients of GP were queried in the TCMSP database, while the names of genes corresponding to the targets were queried in the UniProt Protein Resource[39] (Uniprot, https://www.uniprot.org/) database.

The keywords "Knee osteoarthritis" were used to collect KOA-related target genes in Online Mendelian Inheritance in Man[40] (OMIM, https://www.omim.org/) database, the DisGeNet[41] (https://www.disgenet.org/) database and the Gene Cards[42] (https://www.genecards.org/) database. This study explored the mechanisms by which GP treats KOA after topical administration, therefore, target genes are those expressed in the skin. The human protein atlas[43] (https://www.proteinatlas.org/humanproteome/tissue) database was used to identify the relevant target genes in the skin. The overlap between effective target genes of the active ingredients of GP and disease target genes in the skin were identified using the Venn Diagram (Origin 2021 plug-in).

To explore the interactions between target proteins, the intersecting target genes were imported into the String database[44] (https://cn.string-db.org/) to obtain the interrelationship network of all proteins. The downloaded protein interactions were imported into the Cytoscape software (3.9.1)[45] to generate a visual representation of the protein-protein interaction (PPI) network.

Intersection target genes were imported into MetaScape[46] (Cytoscape 3.9.1 plug-in) and set to $p < 0.05$.[47] Subsequently, the resulting dataset was subjected to an analysis of GO and KEGG pathway enrichment. Specifically, the GO Biological Processes, GO Molecular Functions, Go Cellular Components, and KEGG pathway options were selected for this analysis.

2.8. Integrated analysis

Intersecting target genes and biomarkers from the Metabolomics and network pharmacology analyses were imported into MetScape[48] (Cytoscape 3.9.1 plug-in) for co-analysis to obtain the key targets, metabolites and the associated pathways.

2.9. Statistical analysis

Data are presented as mean ± standard deviation and were analyzed using the SPSS (v25.0) software. Comparisons of means between groups was performed using the t-test, with $p < 0.05$ being the threshold for statistical significance and $p < 0.01$ indicating highly significant differences.

3. Results

3.1. Histopathological analysis

The knee joint cartilage surface in the CON group exhibited an intact structure, with layers of normal chondrocytes. In contrast, the structure

of knee joint cartilage in the MOD group was disorganized, and its chondrocytes had abnormal morphology. Moreover, multiple cases of angiogenesis were observed, signifying an abnormal inflammatory response. Inflammation in the GP group was improved to some extent, the cartilage surfaces were slightly rough.

3.2. Biochemical analysis

Fig. 3A shows that plasma IL-4 levels were significantly lower, while IL-6 and IL-17 levels were significantly higher in the MOD group relative to the CON group. On day 7, joint swelling reached the peak (Fig. 4A), whereas dietary intake and activity levels were decreased. These results and those of histopathological observation implied confirmed the successful establishment of KOA models.

Fig. 3 Aand B shows that the levels of inflammatory factors were comparable to those in the CON group after GP treatment. Levels of neurotransmitters (CGRP, SP, and 5-HT) in skin tissues of the MOD group were significantly higher relative to those of the CON group. After GP administration, neurotransmitter levels were markedly decreased in the GP group, but were significantly higher than those in the CON group. This shows that KOA induces changes in expressions of neurotransmitters in skin tissues, and that GP administration upregulates the levels of neurotransmitters in the skin. There were significant correlations between plasma inflammatory factors and knee skin tissue neurotransmitters (Fig. 4C). Neurotransmitters were negatively correlated with IL-4 but were positively correlated with IL-6 and IL-17. This suggests that GP-mediated regulation of neurotransmitter levels in skin tissues is closely linked to KOA treatment.

3.3. Metabolomic profiling

Fig. 4A shows that TIC peak retention times and peak areas of QC samples exhibit significant overlaps. Table S2 provides evidence of the instrument's stability, as the internal standard displays peak area RSD ≤30 % in QC samples.

The PLS-DA model was used to analyze three groups of data samples. Samples from the same group tended to cluster together. The model also showed that the CON and MOD groups (Fig. 5B) were completely separated, implying that KOA led to skin metabolic disorders. The GP group was entirely separated from the MOD group but was relatively close to the CON group (Fig. 5C), indicating that GP regulated the KOA-induced skin metabolic disorders. The model parameters R^2Y and Q^2 were used to evaluate the explanatory and predictive rates of PLS-DA, respectively. A model was considered reliable if both the R^2Y and Q^2 values were above 0.5 and their difference remained within 0.3. Higher values closer to 1 indicated a stronger model. The lower the model parameters are, the worse the fitting accuracy of the model is.[49,50] In the PLS-DA score plot, R^2Y was 0.997 and 0.993, while Q^2 was 0.839 and

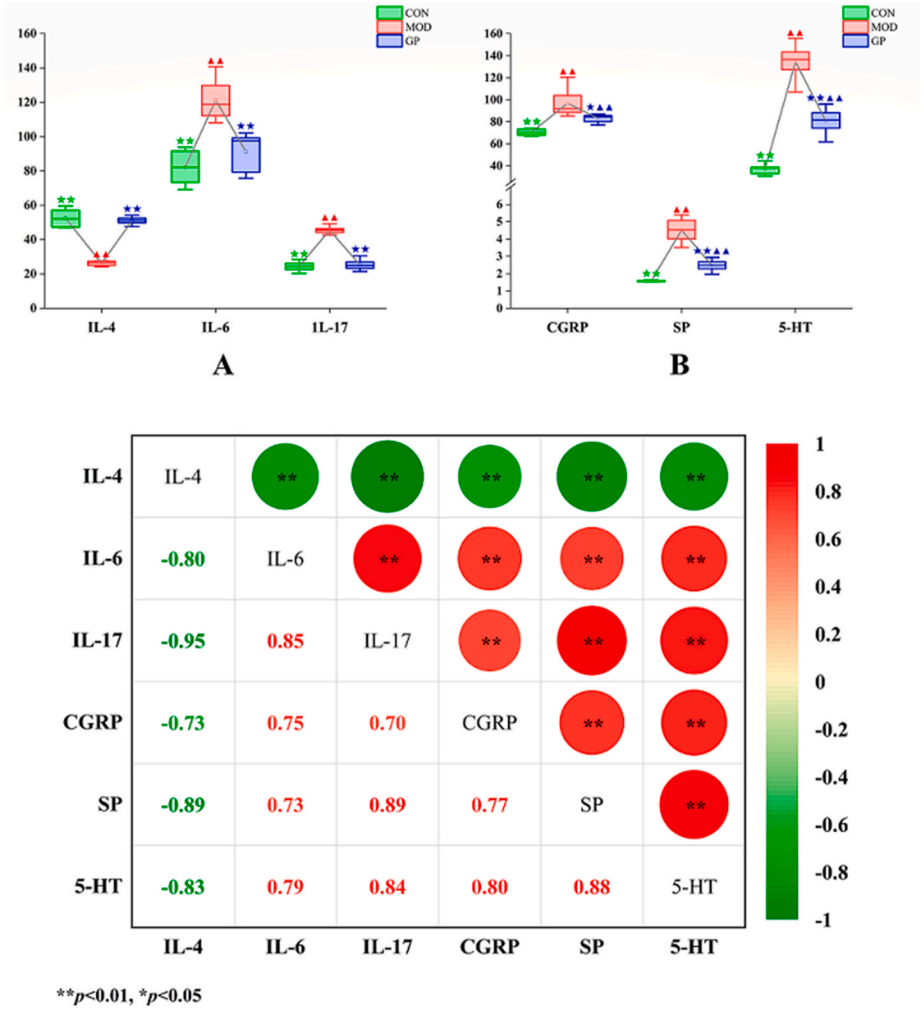

Fig. 3. Results of biochemical analysis: (A) Skin tissue neurotransmitter levels (B) Plasma inflammatory factor levels (C) Correlation analysis. Note: In (A) and (B), compared with CON, $^{▲}p < 0.05$, $^{▲▲}p < 0.01$, compared with MOD group, $^{★}p < 0.05$, $^{★★}p < 0.01$.

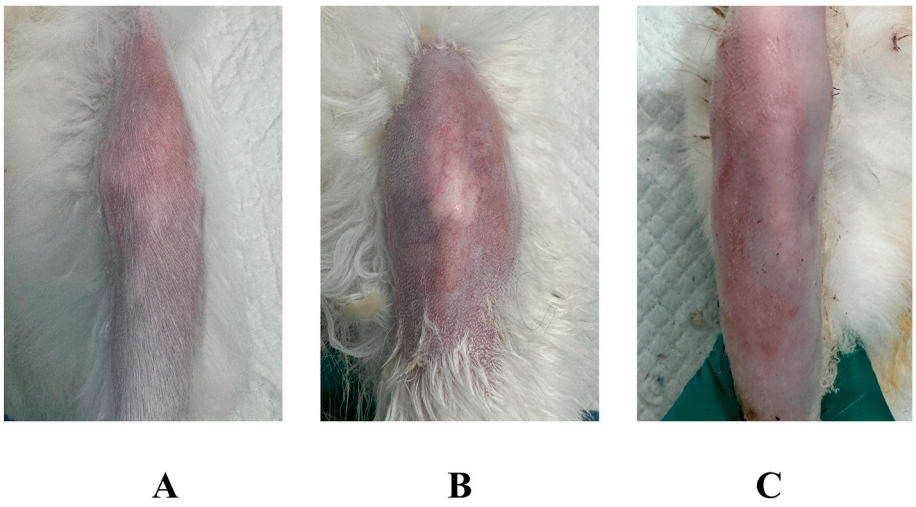

Fig. 4. Knee joints of different groups: (A) CON group (B) MOD group (C) GP group.

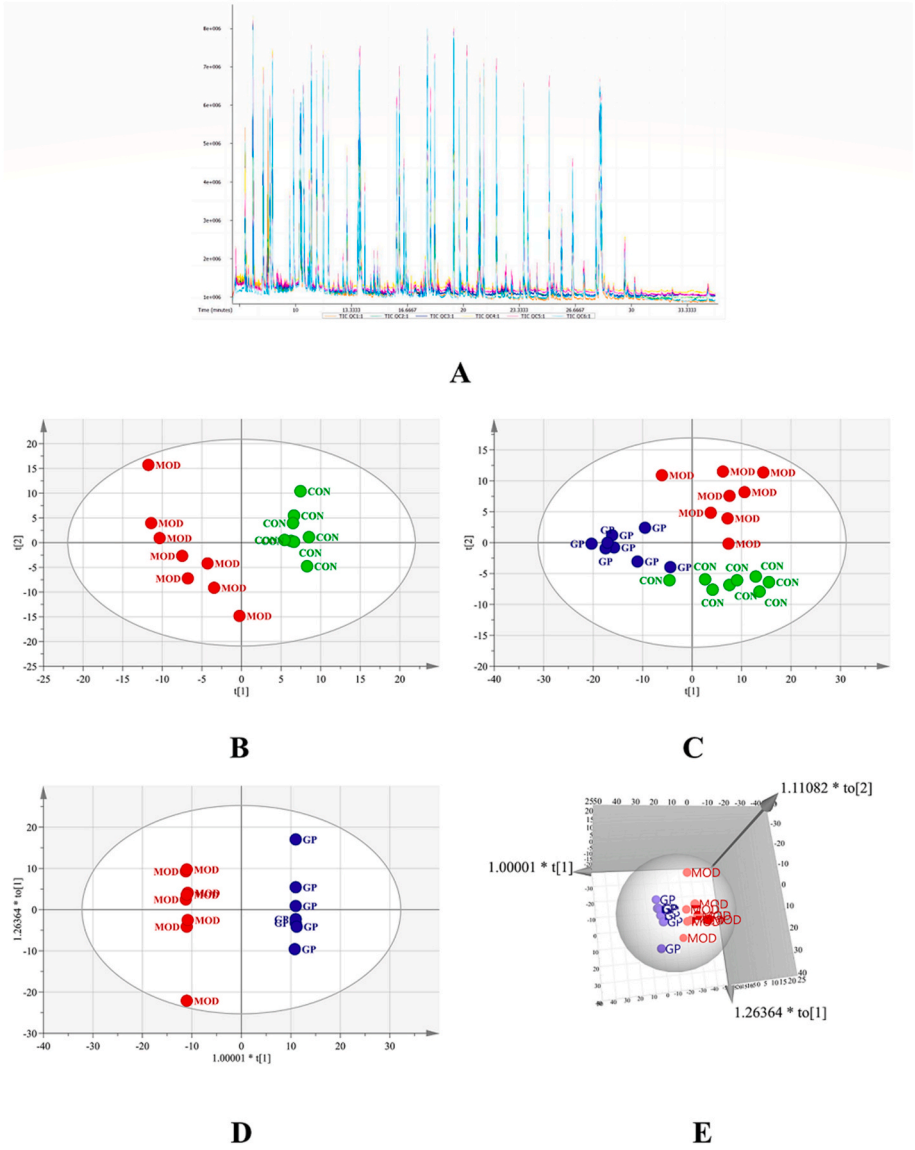

Fig. 5. Metabolomic analyses: (A) TIC stacked plot of QC samples. (B) PLS-DA score plot of CON and MOD groups. (C) PLS-DA score plot of 3 groups. (D) OPLS-DA score plot of GP and MOD groups. (E) OPLS-DA of GP and MOD groups 3D graph.

0.880, respectively, indicating that stability and predictive abilities of the model were good. In the PLS-DA score plots, R^2Y is 0.997 and 0.993, and Q^2 is 0.839 and 0.880, and their values are higher than 0.5 and the differences are not more than 0.3, which indicate that the model had good prediction performance.

3.4. Differentially expressed metabolites and enriched pathways

Differentially expressed metabolites between the MOD and GP groups were screened using the OPLS-DA model ($R^2Y = 1$, $Q^2 = 0.803$) (Fig. 5D and E). A total of 85 differentially expressed metabolites were identified (Table S2), among which 33 were downregulated while 52 were upregulated in the GP group. This shows that topical administration of GP resulted in changes in levels of the above metabolites. Among the altered metabolites, 15 were identified as key markers of KOA. Notably, the expression of these markers was altered in the KOA group, and GP treatment restored their expression. This suggests that topical application of GP directly alters these KOA markers. Specifically, following GP treatment, 10 markers were decreased and 5 were upregulated.The 85 differentially expressed metabolites were imported into MetaboAnalyst for enrichment analysis. They were found to be enriched in 16 metabolic pathways (Fig. 6A). The pathways are associated with carbohydrate, amino acid and lipid metabolism (Fig. 6B). These findings indicate that topically administered GP modulated the above metabolic pathways. Fifteen differentially expressed metabolites were introduced into MetaboAnalyst for enrichment analyses to investigate the mechanisms involved in therapeutic effects of GP against KOA. Six metabolic pathways (Fig. 6C) were associated with the mechanisms of GP. These pathways are involved in carbohydrate and amino acid metabolism (Fig. 6D), implying that GP alleviates KOA by modulating the above metabolic pathways in the skin.

Cluster heat map analysis was performed to visualize the therapeutic effects of the 85 differentially expressed metabolites. Fig. 7A shows that levels of the 85 differentially expressed metabolites were downregulated to varying degrees in the GP group, compared to the MOD group. Studies have reported that GP regulates three metabolic pathways: carbohydrate metabolism, amino acid metabolism and lipid metabolism, resulting in changes in levels of the above 85 metabolites in the skin.

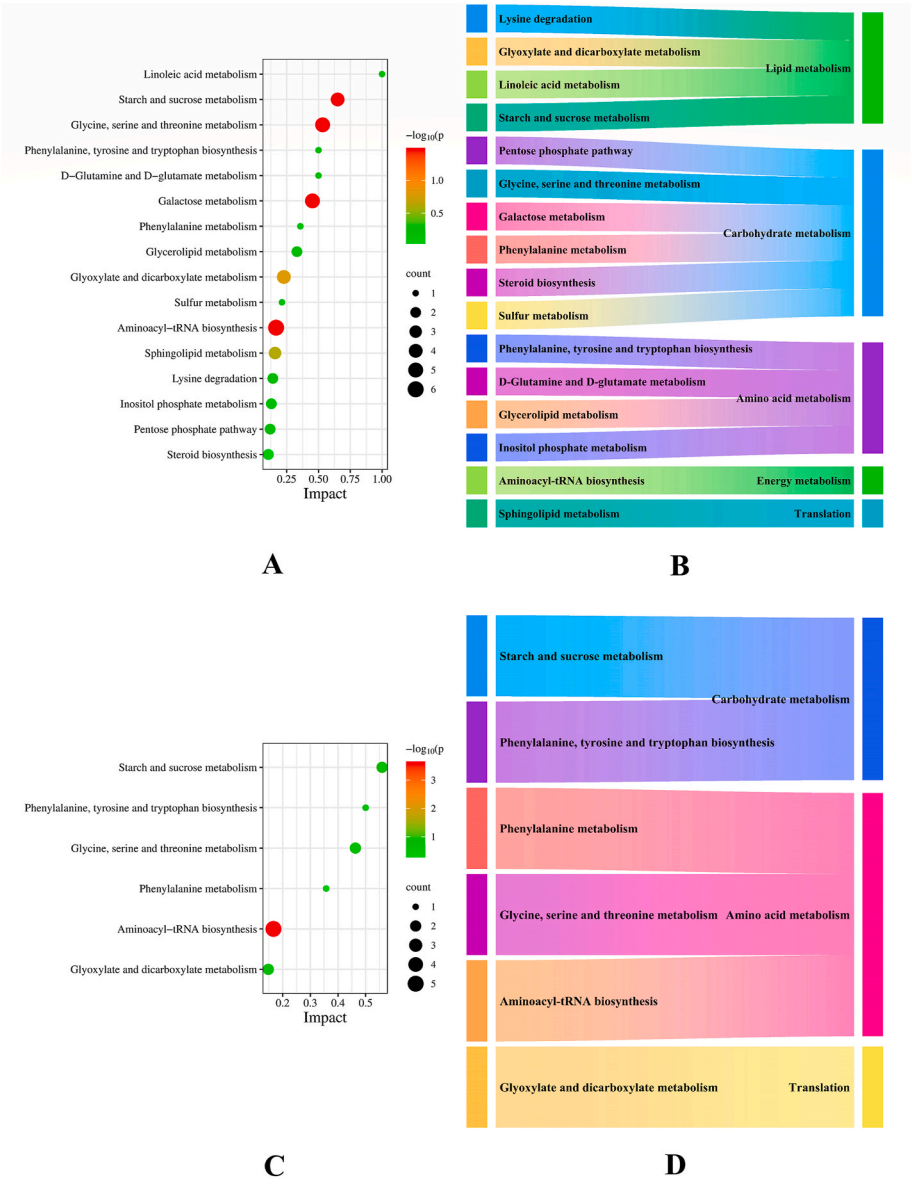

Fig. 6. Pathway and efficacy analyses: (A) Bubble plots of 85 differentially expressed metabolites in the KEGG pathway enrichment analysis (B) The KEGG pathway enrichment analysis show in the major pathways associated with 85 differentially expressed metabolites (C) Bubble plots of 15 biomarkers in the KEGG pathway enrichment analysis (D) Major pathway attribution of 15 biomarkers in the KEGG pathway enrichment analysis.

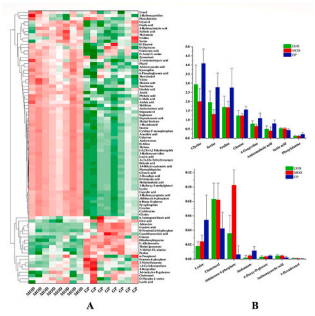

Fig. 7. Analysis of efficacy: (A) The effect of GP on the skin following topical administration (B) Therapeutic effect of GP on KOA.

Among the 15 biomarkers, biomarker levels were significantly upregulated or downregulated in the MOD group, compared to the CON group, and 15 biomarkers tended to return to normal levels after GP administration (Fig. 7B). This demonstrates that GP can treat KOA by restoring the two pathways that modulate carbohydrate metabolism and amino acid metabolism in the skin.

3.5. Network pharmacological analysis

A total of 531 active ingredients were selected from 29 Chinese herbal medicines. Then, 719 targets corresponding to active ingredients and 1385 KOA-related disease targets were screened from databases. A total of 217 KOA targets for 353 active ingredients in GP were screened out, 181 of which were expressed in the skin (Fig. 8A). Finally, we

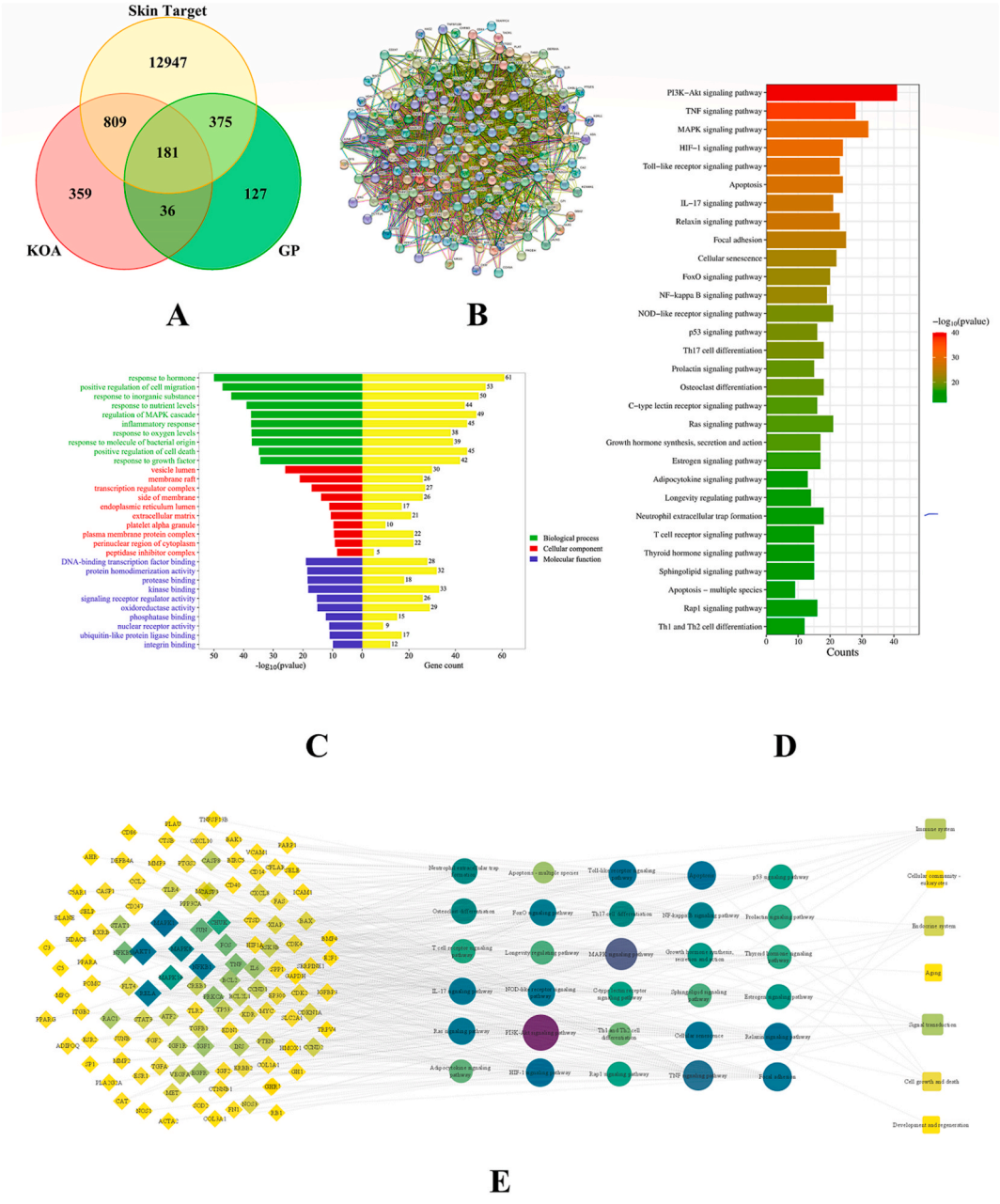

Fig. 8. Network pharmacology analysis: (A) Venn diagram of KOA-GP active compound intersecting skin targets (B) PPI network: edges with different colors represent different associations, 181 target proteins are closely related to each other and may be involved in multiple pathways (C) GO analyses (D) KEGG pathway analysis (E) Target-KEGG pathway-pathway type network: diamonds represent 181 intersecting targets, circles represent 30 KEGG pathways for enrichment analysis, and squares represent 7 pathway attributions, with nodes indicating larger degree values and darker color for larger nodes.

obtained 181 skin targets for GP in KOA. The obtained targets were imported into the Srting database to establish a PPI network of targets (Fig. 8B). The network contained 181 nodes and 4171 edges.

The targets were imported into the Metascape analysis platform for GO and KEGG analyses. The top 10 targets with the smallest *p*-value were selected for graph presentation (Fig. 8C). A total of 2134, 102 and 177 entries were found to be enriched in BP, and CC and MF, respectively. There were 207 KEGG-enriched pathways. The first 30 relevant pathways, including the PI3K-Akt signaling pathway, TNF signaling pathway, HIF-1 signaling pathway, MAPK signaling pathway, Toll-like receptor signaling pathway, apoptosis, relaxin signaling pathway, IL-17 signaling pathway, focal adhesion, cellular senescence, NF-kappa B signaling pathway, FoxO signaling pathway, Th17 cell differentiation, p53 signaling pathway, NOD-like receptor signaling pathway, osteoclast differentiation, prolactin signaling pathway, growth hormone synthesis, secretion and action, ras signaling pathway, C-type lectin receptor signaling type lectin receptor signaling pathway, estrogen signaling pathway, T cell receptor signaling pathway, neutrophil extracellular trap formation, longevity regulating pathway, adipocytokine signaling pathway, sphingolipid signaling pathway, thyroid hormone signaling pathway, Rap1 signaling pathway, apoptosis - multiple species multiple species, Th1 and Th2 cell differentiation were selected and plotted (Fig. 8D) and used to establish the target-KEGG pathway-pathway type network (Fig. 8E). The 30 KEGG pathways are mainly associated with the signaling pathways, immune system, and endocrine system, indicating that topical application of GP can treat KOA by regulating signaling pathways, endocrine and immune systems.

3.6. Integrated analysis of metabolomics and network pharmacology

Fig. 9 shows the interactive network based on metabolomics analyses and network pharmacology. The compound-reaction-enzyme-gene network was established by importing differentially expressed metabolites into MetScape. Through the integration of potential targets identified in network pharmacology with genes from MetScape analysis, three pivotal targets—MPO, CBS, and P4HB—were identified. The key metabolites of interest encompassed L-serine, L-phenylalanine, L-proline, L-lysine, and glycine. The affected pathways were methionine and cysteine metabolism, tyrosine metabolism, urea cycle and metabolism of arginine, proline, glutamate, aspartate and asparagine, respectively (Table S3).

4. Discussion

The pathogenesis of KOA is attributed to cartilage damage that is caused by uneven joint stress distribution.[51] We used a combination of cold stimulation and drug induction to establish KOA models. By combining ice water bath stimulation with papain injection, type II collagen levels in the cartilage were reduced,[52,53] resulting in degeneration and damage of articular cartilage, soft tissue inflammation and ossification and knee swelling.[54] In this study, joint swelling reached the peak value (Fig. 4), while dietary intake and activity levels were reduced. Moreover, cartilage damage was enhanced and inflammatory factor levels were elevated, demonstrating the successful establishment of the KOA models.

Histopathological and biochemical analyses (Figs. 2, 3A and 3B)

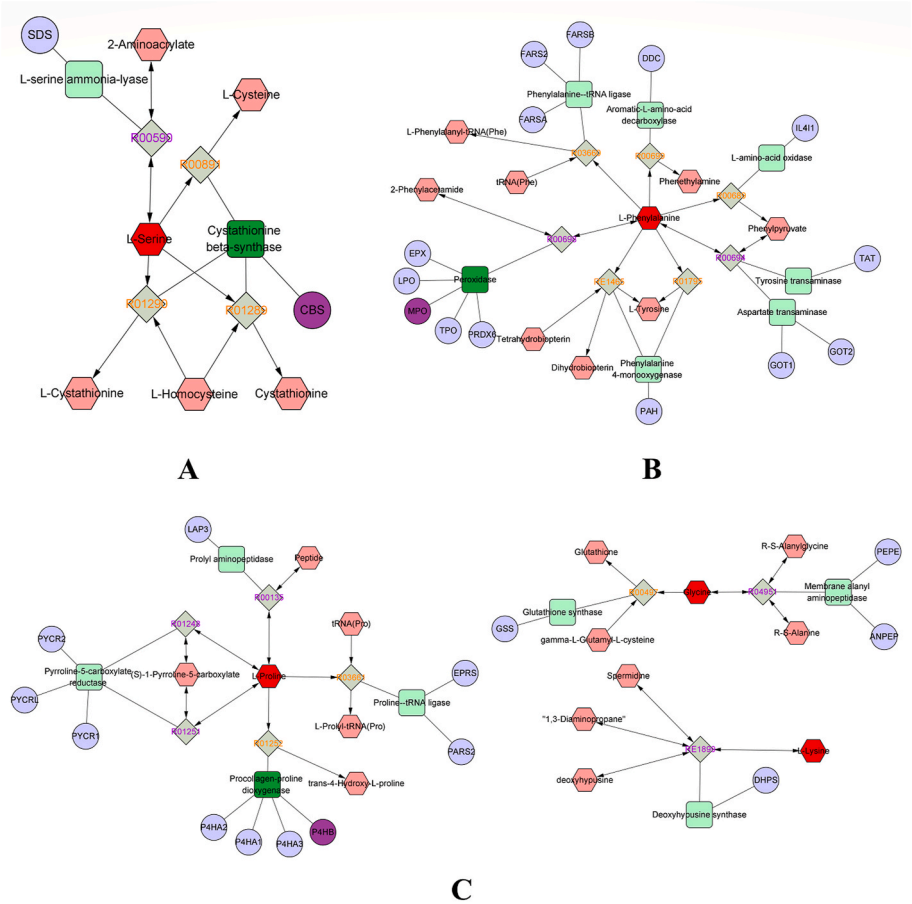

Fig. 9. Compound-reaction-enzyme-gene networks for key metabolites and targets: red hexagons, grey diamonds, green rounded rectangles and purple circles represent active ingredients, reactions, proteins and genes respectively and key metabolite, protein and gene colors are weighted. (A) Methioine and cysteine metabolism (B) Tyroine metabolism (C) Urea cycle and metabolism of arginine, proline, glutamate, aspartate and asparagine.

revealed that articular cartilage structures in the MOD group were completely destroyed, and there was inflammation accompanied by significant changes in plasma levels of inflammatory factors (IL-4, IL-6, and IL-17) and neurotransmitter (CGRP, SP and 5-HT) levels in knee skin tissues. After GP administration, articular cartilage structures recovered, inflammation was alleviated, while levels of plasma inflammatory factors were restored to levels that were comparable to those of the CON group. Neurotransmitter levels in knee skin tissues were reduced and remained relatively high. There were significant correlations (Fig. 3C) between GP plasma inflammatory factor levels and knee skin tissue neurotransmitter levels, suggesting that GP exerts its therapeutic effects by modulating neurotransmitters in the skin. We found that KOA deregulates skin carbohydrate and amino acid metabolism, as revealed by significant changes in levels of 15 biomarkers (Table S2). This is consistent with the TCM theory of acupoint sensitization. It involves the activation of endogenously regulated biological programs triggered by inflammatory factors at acupuncture points. These areas exhibit neurogenic inflammatory responses within the organism under pathological conditions.[55] A metabolomics study indicated that the content of metabolites such as histidine, glutamate, phenylalanine, and 3-hydroxy acid in the subcutaneous microdialysis fluid of rabbits with myocardial ischemia model was significantly different from that of the blank group, which may be potential myocardial ischemia acupoint markers.[56] After GP administration, levels of the 15 biomarkers (Table S2) were reversed by regulating skin carbohydrate, amino acid and lipid metabolism (Fig. 6C and D). Levels of 70 differentially expressed metabolites (Table S2) were also changed. Alterations in subcutaneous microdialysis fluid levels of histidine, glutamate, stearic acid, and 3-hydroxyacid following acupuncture administration to rabbits with a myocardial ischemia model indicate that these substances could serve as potential markers for assessing the impact of acupuncture in myocardial ischemia.

The skin is the first line of defense against external environmental aggression.[57] The extracellular space of the epidermis mainly comprises lipids arranged in multilayered bilayers, including free fatty acids, ceramides, and triglycerides.[58] The ceramide structure consists mainly of hydrophobic fatty acid chains linked to amino sphingolipids formed when serine is catalyzed. Linoleic acid, which is a precursor for ceramide synthesis. It can increase tight junctions between cells and maintain the integrity as well as tightness of the skin barrier, thereby protecting and repairing the skin barrier.[59] Previoously, it was observed that increased sphingosine to phytosphingosine ratio affected the skin barrier function.[60] Moreover, changes in lipids, like linoleic acid, and amino acids, like serine, in skin metabolomics studies, may indicate metabolic disruption and imparired skin barrier function.[61] In this study, phytosphingosine, linoleic acid, and cholesterol levels in the GP group were up-regulated while serine and DL-dihydrosphingosine levels were down-regulated, implying that GP affects epidermal lipid metabolism, regulates skin structure changes,[62,63] accelerates material exchange as well as skin barrier transport, and promotes osmotic drug absorption. This conclusion is similar to the concept of “opening and closing of the striae” effect in TCM theory.

Purines and adenosine triphosphate (ATP) are key components of the cellular energy system.[64] Acupuncture treatment triggers the release of purines, key energy molecules within cells. Enzymes then convert these purines into specific signaling molecules, acting as messengers that travel to the spinal cord and brain, ultimately coordinating the body’s response.[65,66] Acupuncture was shown to increase the extracellular concentrations of ATP, adenosine monophosphate (AMP) and adenosine (ADO) in tissues of Zusanli in mice, acting on adenosine receptor A_1 and thereby exerting analgesic effects.[67] In this study, xanthine, inosine and ADO levels were upregulated after GP administration, implying the activation of local signaling to stimulate the release of large amounts of purine signaling molecules from keratin-forming cells, fibroblasts and other types of cells in the skin. These effects result in activation of ion channel receptors of purine signaling receptors on sensory nerves in the skin, which transmit information to the brainstem and hypothalamus via the sensory ganglia and spinal cord, making the corresponding reflexes to release the corresponding substances or signals to the corresponding parts of the body, leading to appropriate responses and therapeutic effects.

Prostaglandin-Endoperoxide Synthase (PTGS)1, PTGS2, peroxisome proliferator-activated receptor gamma (PPARG) and B-cell lymphoma (Bcl)-2 were identified in a network pharmacology study that aimed to explore the application of Sinomenium diversifolium Diels in the treatment of KOA. Wenyujin Rhizoma Concisum-Angelica Sinensis Radix for the treatment of KOA.[68] In another network pharmacology study, the key targets of Cathepsin K (CTSK), PTGS1 and PTGS2 were identified78. In this study, 217 targets GP in the treatment of KOA were predicted, which included PTGS1 and PTGS2 identified in previous studies. In addition, special skin targets were screened, such as Cystathionine beta synthase (CBS). By combining the metabolomics results with that of network pharmacology, we identified 3 key targets, 5 key metabolites and 3 related pathways (Table S3).

CBS promotes the synthesis of cystathionine, a metabolic intermediate of the sulphur-containing amino acids, from serine and homocysteine (Hcy). Activation of CBS causes abnormalities in the metabolism of sulphur-containing amino acids and affects levels of the important human metabolite glutathione. Glutathione plays a crucial role in the body by scavenging hyperoxide ions and various free radicals. It promotes the integrity of cell membranes, guards against lipid oxidation, enhances the defensive capabilities of macrophages against bacterial intrusion, and contributes to the regulation of T-cell immunity.[69] In nerve cells, CBS catalyzes the synthesis of hydrogen sulfide (H_2S) from L-cysteine.[70] H_2S is the third novel biogas signaling molecule after nitric oxide (NO) and carbon monoxide (CO), known to be involved in the regulation of the body’s immune function, physiological functions, and pathological processes of the body such as the cardiovascular system and the nervous system.[71–74] In brain tissue, H_2S can act as a neurotransmitter or neuromodulator, exerting a variety of biological effects, such as the modulation of learning and memory functions by promoting hippocampus development over long periods of time, inhibition of neuroinflammatory responses and strong neuroprotective effects via reducing anti-oxidative stress damage and anti-apoptotic cell death.[75,76] Studies have demonstrated a negative correlation between the imaging stage of knee osteoarthritis and the expression level of H_2S in the synovial fluid of affected patients.[77] It has also been reported that GP may exert a therapeutic effect on KOA by acting on CBS in skin nerve cells to catalyze the synthesis of H_2S.

Myeloperoxidase (MPO), also known as peroxidase, is involved in the phenylalanine metabolism. Phenylalanine is a precursor of catecholamine neurotransmitters and tyrosine. It can synthesize proteins needed by cells such as tyrosine as well as neurotransmitters and hormones. Studies have demonstrated that dopamine (DA) neurotransmitters can inhibit PI3K/Akt signaling, affect NF-κB signaling and down-regulate the expression of metalloproteinases (MMP) in articular chondrocytes in KOA rats.[78] Activation of MPO resulted in down-regulation of phenylalanine expression, indirectly impairing the conversion of phenylalanine to tyrosine and catecholamine synthesis, suggesting that neurotransmitter disorders in the skin tissue of KOA rabbits may contribute to the regulation of amino acid metabolism.

The hydroxyproline produced through post-translational modification of proline by prolyl 4-hydroxylase (P4HB) is a major component of collagen and its deficiency decreases the structural stability of the collagen triple helix,[79] and hence the overall collagen synthesis. Proline levels were upregulated in the skin tissue of KOA rabbits, suggesting that proline hydroxylation was blocked and collagen synthesis was affected. Collagen in the extracellular matrix of the dermis provides attachment points and mechanical resistance required to keep the skin fibers intact, and is involved in and induces cell behaviors that facilitate cell differentiation and promote wound healing and tissue regeneration. Compared with the CON group, the levels of proline, glycine and lysine in the MOD group were significantly up-regulated, while those in the GP

group were significantly down-regulated. This demonstrated impaired collagen synthesis in the skin following KOA. GP treatment restored amino acid metabolism in the skin tissue and exerted a therapeutic effect on KOA.

In this study, the therapeutic effect and mechanism of GP, a traditional Chinese medicine preparation, on KOA was explored. Moreover, its effect on skin was verified. We identified key targets and pathways for further investigation. Lack of experimental validation is one of the limitations of this study. Our results suggest that the therapeutic mechanism of GP may be similar to that of acupuncture and moxibustion, and it may have broad effects beyond those elicited by its active ingredients. Integrating this mechanism with other topical agents provides a new idea for the design and exploration of modern topical agents.

5. Conclusion

The results in the present study suggest that the therapeutic effects of GP is associated with suppression of proinflammatory cytokines and neurotransmitters, skin lipid and amino acid metabolism, and the purinergic signaling pathway. Further experiments to directly measure these metabolites are needed to verify the findings. The findings in this study provide new insights into the mechanism underlying the beneficial effects of GP in the treatment of KOA and also provides a new perspective for exploring the pharmacological mechanism of TCM preparations.

Ethics approval and consent to participate

The Animal Care and Ethics Committee at Heilongjiang University of Chinese Medicine approved this study, which was performed in accordance with the NIH Guidelines for Care and Use of Laboratory Animals (USA).

Taxonomy

The experimental approach.

Consent for publication

All authors have read the manuscript and approved its submission.

Availability of data and material

The datasets used or analyzed during the current study are available from the corresponding author on reasonable request.

Declaration of competing interest

The authors declare that they have no known competing financial interests or personal relationships that could have appeared to influence the work reported in this paper.

Acknowledgments

The present study was supported by the National Natural Science Foundation of China (Grant approval No. 82074025), the Chinese Medicine Research Project of Heilongjiang Provincial Administration of Traditional Chinese Medicine (ZHY2023-017) and Heilongjiang Touyan Innovation Team Program.

Appendix A. Supplementary data

Supplementary data to this article can be found online at https://doi.org/10.1016/j.jtcme.2024.04.004.

References

1. Lespasio MJ, Piuzzi NS, Husni ME, Muschler GF, Guarino A, Mont MA. Knee osteoarthritis: a Primer. *Perm J*. 2017;21:16–183. https://doi.org/10.7812/TPP/16-183.
2. Li D, Li S, Chen Q, Xie X. The prevalence of Symptomatic knee osteoarthritis in relation to age, Sex, area, region, and body mass index in China: a systematic review and meta-analysis. *Front Med*. 2020;7:304. https://doi.org/10.3389/fmed.2020.00304.
3. Driban JB, Bannuru RR, Eaton CB, et al. The incidence and characteristics of accelerated knee osteoarthritis among women: the Chingford cohort. *BMC Muscoskel Disord*. 2020;21(1):60. https://doi.org/10.1186/s12891-020-3073-3.
4. Pharmacopoeia Commission. *Pharmacopoeia of People's Republic of China: IV*. 11 ed. China Medical Sciences Press; 2020.
5. Xue Y, Guan T, Liu J, et al. Chemical composition analysis and multi-index component content determination of compounds in Goupi plaster based on UPLC–Q-exactive-MS and UPLC–MS/MS. *Chromatographia*. 2023. https://doi.org/10.1007/s10337-023-04296-7. Published online November 20.
6. Chern CM, Zhou H, Wang YH, et al. Osthole ameliorates cartilage degradation by downregulation of NF-κB and HIF-2α pathways in an osteoarthritis murine model. *Eur J Pharmacol*. 2020;867, 172799. https://doi.org/10.1016/j.ejphar.2019.172799.
7. Huang Z, Mao X, Chen J, et al. Sinomenine hydrochloride injection for knee osteoarthritis: a protocol for systematic review and meta-analysis. *Medicine (Baltim)*. 2022;101(2), e28503. https://doi.org/10.1097/MD.0000000000028503.
8. Wu Y, Lin Z, Yan Z, Wang Z, Fu X, Yu K. Sinomenine contributes to the inhibition of the inflammatory response and the improvement of osteoarthritis in mouse-cartilage cells by acting on the Nrf2/HO-1 and NF-κB signaling pathways. *Int Immunopharm*. 2019;75, 105715. https://doi.org/10.1016/j.intimp.2019.105715.
9. Hou XT, Hao EW, Qin JF, et al. Chemical components and pharmacological action for Cinnamomum cassia and predictive analysis on Q-marker. *Chin Tradit Herb Drugs*. 2018;49(1):20–34.
10. Liu S, Wang WY, Wang YC, Xu KY, Xu DD, Teng JL. Pharmacodynamic material basis of Astragali Radix and Angelicae Sinensis Radix drug pair in supplementing Qi and activating blood circulation. *Chin J Exp Tradit Med Formulae*. 2023;29(9):28–36. https://doi.org/10.13422/j.cnki.syfjx.20230412.
11. Wang JJ, Liu ZH, Zhang QQ, Wang R, Wang YH, Li YJ. Research progress of Goupi plaster. *Acta Chin Med Pharmacol*. 2022;50(4):109–114. https://doi.org/10.19664/j.cnki.1002-2392.220095.
12. Ge H. *The Handbook of Prescriptions for Emergencies*. China of Press Traditional Chinese Medicin; 2016.
13. Wang JJ, Zhu T, Liu ZH, Wang YH, Li YJ. Study on the vascular reactivity of Black Plaster on rabbits with osteoarthritis model with cold clotting and blood stasis based on the theory of "opening and closing the couples.". *Eval Anal Drug-Use Hosp China*. 2022;22(4):401–406. https://doi.org/10.14009/j.issn.1672-2124.2022.04.004.
14. Sun HT, Xie GP, Li FM, Lin ZS, Li QH. Clinical observation on the treatment of knee osteoarthritis with external application of Goupi Plaster combined with quadriceps endurance training. *Yunnan J Tradit Chin Med*. 2014;35(6):52–53. https://doi.org/10.16254/j.cnki.53-1120/r.2014.06.054.
15. Miller K. Transdermal patches: past, present and future. *Ther Deliv*. 2015;6(6):639–641. https://doi.org/10.4155/tde.15.16.
16. Tian S, Miao MS. Exploring the mechanism of topical action of traditional Chinese medicine based on neuro-endocrine-immune network-"three micro-regulation balance". *Chin J Exp Tradit Med Formulae*. 2019;25(4):6–12. https://doi.org/10.13422/j.cnki.syfjx.20190436.
17. Yuan HD, Ma QQ, Cui HY, et al. How can synergism of traditional medicines benefit from network pharmacology? *Molecules*. 2017;22(7):1135. https://doi.org/10.3390/molecules22071135.
18. Johnson CH, Ivanisevic J, Siuzdak G. Metabolomics: beyond biomarkers and towards mechanisms. *Mol Cell Biol*. 2016;17(7):451–459. https://doi.org/10.1038/nrm.2016.25.
19. Von Kaeppler EP, Wang Q, Raghu H, Bloom MS, Wong H, Robinson WH. Interleukin 4 promotes anti-inflammatory macrophages that clear cartilage debris and inhibits osteoclast development to protect against osteoarthritis. *Clin Immunol*. 2021;229, 108784. https://doi.org/10.1016/j.clim.2021.108784.
20. Tang J, Zhou Z, Xiao J, Gao Z, Zuo J. Research progression in the pathogenesis of osteoarthritis. *China J Orthop Traumatol*. 2021;34(10):985–990.
21. Kim EK, Kwon JE, Lee SY, et al. IL-17-mediated mitochondrial dysfunction impairs apoptosis in rheumatoid arthritis synovial fibroblasts through activation of autophagy. *Cell Death Dis*. 2017;8(1), e2565. https://doi.org/10.1038/cddis.2016.490.
22. He W, Wang XY, Shi H, et al. Cutaneous neurogenic inflammation in the sensitized acupoints induced by gastric mucosal injury in rats. *BMC Compl Alternative Med*. 2017;17(1):141. https://doi.org/10.1186/s12906-017-1580-z.
23. Chen S, Zhang GY, Wang YY, et al. Effect of moxibustion and scraping on bioactive substances changes of acupoints in knee osteoarthritis rats. *Zhen Ci Yan Jiu*. 2023;48(4):359–365. https://doi.org/10.13702/j.1000-0607.20220994.
24. Wang X, Shen F. [Effects of mechanical ventilation with different tidal volumes on coagulation/fibrinolysis in rabbits with acute respiratory distress syndrome]. *Zhonghua Wei Zhong Bing Ji Jiu Yi Xue*. 2015;27(7):585–590. https://doi.org/10.3760/cma.j.issn.2095-4352.2015.07.009.
25. Bu T, Zhang M, Lee SH, et al. GC-TOF/MS-Based metabolomics for comparison of volar and non-volar skin types. *Metabolites*. 2022;12(8):717. https://doi.org/10.3390/metabo12080717.
26. Zhang S, Zhang X, Sun G, et al. Tuina intervention in rabbit model of knee osteoarthritis. *J Vis Exp*. 2023;198. https://doi.org/10.3791/65763.

27. Pan Z, Lin H, Fu Y, et al. Identification of gene signatures associated with ulcerative colitis and the association with immune infiltrates in colon cancer. *Front Immunol*. 2023;14, 1086898. https://doi.org/10.3389/fimmu.2023.1086898.
28. Poole CF. Evaluation of the solvation parameter model as a quantitative structure-retention relationship model for gas and liquid chromatography. *J Chromatogr A*. 2020;1626, 461308. https://doi.org/10.1016/j.chroma.2020.461308.
29. Lopes AS, Cruz ECS, Sussulini A, Klassen A. Metabolomic strategies involving mass spectrometry combined with liquid and gas chromatography. *Adv Exp Med Biol*. 2017;965:77–98. https://doi.org/10.1007/978-3-319-47656-8_4.
30. Nipun TS, Khatib A, Ibrahim Z, et al. GC-MS- and NMR-based metabolomics and molecular docking reveal the potential alpha-glucosidase inhibitors from Psychotria malayana Jack Leaves. *Pharmaceuticals*. 2021;14(10):978. https://doi.org/10.3390/ph14100978.
31. Saccenti E, Hoefsloot HCJ, Smilde AK, Westerhuis JA, Hendriks MMWB. Reflections on univariate and multivariate analysis of metabolomics data. *Metabolomics*. 2014;10(3):361–374. https://doi.org/10.1007/s11306-013-0598-6.
32. Song L, Yin Q, Kang M, et al. Untargeted metabolomics reveals novel serum biomarker of renal damage in rheumatoid arthritis. *J Pharm Biomed Anal*. 2020;180, 113068. https://doi.org/10.1016/j.jpba.2019.113068.
33. Wishart DS, Guo A, Oler E, et al. Hmdb 5.0: the human Metabolome database for 2022. *Nucleic Acids Res*. 2021;50(D1):D622–D631. https://doi.org/10.1093/nar/gkab1062.
34. Huckvale E, Moseley HNB. kegg_pull: a software package for the RESTful access and pulling from the Kyoto Encyclopedia of Gene and Genomes. *BMC Bioinf*. 2023;24(1):78. https://doi.org/10.1186/s12859-023-05208-0.
35. Chong J, Wishart DS, Xia J. Using MetaboAnalyst 4.0 for comprehensive and integrative metabolomics data analysis. *Curr Protoc Bioinformatics*. 2019;68(1), e86. https://doi.org/10.1002/cpbi.86.
36. Wang W, Li M, Si H, Jiang Z. Network pharmacology and integrated molecular docking study on the mechanism of the therapeutic effect of Fangfeng decoction in osteoarthritis. *Curr Pharmaceut Des*. 2023;29(5):379–392. https://doi.org/10.2174/1381612829666230216095659.
37. Ru J, Li P, Wang J, et al. TCMSP: a database of systems pharmacology for drug discovery from herbal medicines. *J Cheminf*. 2014;6:13. https://doi.org/10.1186/1758-2946-6-13.
38. Fang S, Dong L, Liu L, et al. HERB: a high-throughput experiment- and reference-guided database of traditional Chinese medicine. *Nucleic Acids Res*. 2021;49(D1):D1197–D1206. https://doi.org/10.1093/nar/gkaa1063.
39. UniProt Consortium. UniProt: the universal protein knowledgebase in 2021. *Nucleic Acids Res*. 2021;49(D1):D480–D489. https://doi.org/10.1093/nar/gkaa1100.
40. Amberger JS, Hamosh A. Searching online Mendelian inheritance in man (OMIM): a knowledgebase of human genes and genetic phenotypes. *Curr Protoc Bioinformatics*. 2017;58(1.2.1-1.2.12). https://doi.org/10.1002/cpbi.27.
41. Piñero J, Saüch J, Sanz F, Furlong LI. The DisGeNET cytoscape app: exploring and visualizing disease genomics data. *Comput Struct Biotechnol J*. 2021;19:2960–2967. https://doi.org/10.1016/j.csbj.2021.05.015.
42. Rappaport N, Fishilevich S, Nudel R, et al. Rational confederation of genes and diseases: NGS interpretation via GeneCards, MalaCards and VarElect. *Biomed Eng Online*. 2017;16(Suppl 1):72. https://doi.org/10.1186/s12938-017-0359-2.
43. Bozoky B, Szekely L, Ernberg I, Savchenko A. AtlasGrabber: a software facilitating the high throughput analysis of the human protein atlas online database. *BMC Bioinf*. 2022;23(1):546. https://doi.org/10.1186/s12859-022-05097-9.
44. Szklarczyk D, Kirsch R, Koutrouli M, et al. The STRING database in 2023: protein-protein association networks and functional enrichment analyses for any sequenced genome of interest. *Nucleic Acids Res*. 2023;51(D1):D638–D646. https://doi.org/10.1093/nar/gkac1000.
45. Otasek D, Morris JH, Bouças J, Pico AR, Demchak B. Cytoscape Automation: empowering workflow-based network analysis. *Genome Biol*. 2019;20(1):185. https://doi.org/10.1186/s13059-019-1758-4.
46. Zhou Y, Zhou B, Pache L, et al. Metascape provides a biologist-oriented resource for the analysis of systems-level datasets. *Nat Commun*. 2019;10. https://doi.org/10.1038/s41467-019-09234-6.
47. Kanehisa M, Furumichi M, Sato Y, Ishiguro-Watanabe M, Tanabe M. KEGG: integrating viruses and cellular organisms. *Nucleic Acids Res*. 2020;49(D1):D545–D551. https://doi.org/10.1093/nar/gkaa970.
48. Karnovsky A, Li S. Pathway analysis for targeted and untargeted metabolomics. *Methods Mol Biol*. 2020;2104:387–400. https://doi.org/10.1007/978-1-0716-0239-3_19.
49. Liu Y, Ma S, Cai Q. Fecal metabonomics study of raw and bran-fried Atractylodis Rhizoma in spleen-deficiency rats. *J Pharm Biomed Anal*. 2020;189, 113416. https://doi.org/10.1016/j.jpba.2020.113416.
50. Hong ZC, Cai Q, Wu HZ, Yang YF, Fan H, Duan XY. Compound Sophorae Decoction: treating ulcerative colitis by affecting multiple metabolic pathways. *Chin J Nat Med*. 2021;19(4):267–283. https://doi.org/10.1016/S1875-5364(21)60029-8.
51. Maly MR, Acker SM, Totterman S, et al. Knee adduction moment relates to medial femoral and tibial cartilage morphology in clinical knee osteoarthritis. *J Biomech*. 2015;48(12):3495–3501. https://doi.org/10.1016/j.jbiomech.2015.04.039.
52. Chen D, Peng LP, Liao ZW, et al. Comparison of papain and plaster braking for establishing a rabbit Knee Osteoarthritis model. *Guangdong Med J*. 2017;38(14):2114–2118. https://doi.org/10.13820/j.cnki.gdyx.20170627.002.
53. Chen ZD, Lin HY, Yu ZY, Li B. Advances in animal models of osteoarthritis of the knee. *Rheumatol Arthritis*. 2016;5(1):67–70.
54. Wu YY, Bai M, Tian S, Miao MS. Animal model analysis of knee osteoarthritis based on clinical characteristics of Chinese and Western medicine. *Zhongguo Zhongyao Zazhi*. 2020;45(11):2481–2485. https://doi.org/10.19540/j.cnki.cjcmm.20200227.403.
55. Xing BB, Huang M, Chen GH, Zhang D, Ding GH. Observation on acupoint sensitization phenomenon in experimental myocardial ischemia rabbits. *Zhen Ci Yan Jiu*. 2017;42(4):327–331.
56. Xing BB, Huang M, Zhang D, Ding GH. Subcutaneous metabolites involving acupoint sensitization induced by myocardial ischemia and acupuncture stimulation in rabbits. *Zhen Ci Yan Jiu*. 2018;43(7):433–439. https://doi.org/10.13702/j.1000-0607.180066.
57. Chambers ES, Vukmanovic-Stejic M. Skin barrier immunity and ageing. *Immunology*. 2020;160(2):116–125. https://doi.org/10.1111/imm.13152.
58. Bhattacharya N, Sato WJ, Kelly A, Ganguli-Indra G, Indra AK. Epidermal lipids: key mediators of atopic dermatitis pathogenesis. *Trends Mol Med*. 2019;25(6):551–562. https://doi.org/10.1016/j.molmed.2019.04.001.
59. Yao QY, Luo Y, Yao X, Liu J. Effect of linoleic acid on the expression of keratin-forming cell barrier-related proteins. *China J Leprosy Skin Dis*. 2019;35(10):584–586+595.
60. Nădăban A, Rousel J, El Yachioui D, et al. Effect of sphingosine and phytosphingosine ceramide ratio on lipid arrangement and barrier function in skin lipid models. *JLR (J Lipid Res)*. 2023;64(8), 100400. https://doi.org/10.1016/j.jlr.2023.100400.
61. Sorokin AV, Domenichiello AF, Dey AK, et al. Bioactive lipid mediator profiles in human psoriasis skin and blood. *J Invest Dermatol*. 2018;138(7):1518–1528. https://doi.org/10.1016/j.jid.2018.02.003.
62. Kendall AC, Kiezel-Tsugunova M, Brownbridge LC, Harwood JL, Nicolaou A. Lipid functions in skin: differential effects of n-3 polyunsaturated fatty acids on cutaneous ceramides, in a human skin organ culture model. *Biochim Biophys Acta*. 2017;1859(9Part B):1679–1689. https://doi.org/10.1016/j.bbamem.2017.03.016.
63. Cha HJ, He C, Zhao H, Dong Y, An IS, An S. Intercellular and intracellular functions of ceramides and their metabolites in skin (Review) *Int J Mol Med*. 2016;38(1):16–22. https://doi.org/10.3892/ijmm.2016.2600.
64. Law KP, Zhang H. The pathogenesis and pathophysiology of gestational diabetes mellitus: deductions from a three-part longitudinal metabolomics study in China. *Clin Chim Acta*. 2017;468:60–70. https://doi.org/10.1016/j.cca.2017.02.008.
65. Burnstock G. Purinergic signaling in the cardiovascular system. *Circ Res*. 2017;120(1):207–228. https://doi.org/10.1161/CIRCRESAHA.116.309726.
66. Tang Y, Yin HY, Rubini P, Illes P. Acupuncture-induced analgesia: a neurobiological basis in purinergic signaling. *Neuroscientist*. 2016;22(6):563–578. https://doi.org/10.1177/1073858416654453.
67. Huang M, Wang X, Xing B, et al. Critical roles of TRPV2 channels, histamine H1 and adenosine A1 receptors in the initiation of acupoint signals for acupuncture analgesia. *Sci Rep*. 2018;8(1):6523. https://doi.org/10.1038/s41598-018-24654-y.
68. Yao RB, Peng H, Cai MC, Li X. Mechanism of Sinomenii caulis in the treatment of rheumatoid arthritis based on network pharmacology. *J pharmace, prac ser*. 2021;39(1):17–22. https://doi.org/10.12206/j.issn.1006-0111.202004117.
69. Mak TW, Grusdat M, Duncan GS, et al. Glutathione primes T cell metabolism for inflammation. *Immunity*. 2017;46(4):675–689. https://doi.org/10.1016/j.immuni.2017.03.019.
70. Feliers D, Lee HJ, Kasinath BS. Hydrogen sulfide in renal physiology and disease. *Antioxidants Redox Signal*. 2016;25(13):720–731. https://doi.org/10.1089/ars.2015.6596.
71. Dilek N, Papapetropoulos A, Toliver-Kinsky T, Szabo C. Hydrogen sulfide: an endogenous regulator of the immune system. *Pharmacol Res*. 2020;161, 105119. https://doi.org/10.1016/j.phrs.2020.105119.
72. Szabo C. Hydrogen sulfide, an enhancer of vascular nitric oxide signaling: mechanisms and implications. *Am J Physiol Cell Physiol*. 2017;312(1):C3–C15. https://doi.org/10.1152/ajpcell.00282.2016.
73. Szabo C, Papapetropoulos A. International union of basic and clinical pharmacology. CII: pharmacological modulation of H_2S levels: H_2S donors and H_2S biosynthesis inhibitors. *Pharmacol Rev*. 2017;69(4):497–564. https://doi.org/10.1124/pr.117.014050.
74. Wang X, Wang S, Chen ZW. Determination of H_2S in rat brain tissue by gas chromatography-mass spectrometry based on bis (pentafluorobenzyl) sulfide. *Chin Pharmacol Bull*. 2022;38(7):1114–1120.
75. Ghanbari F, Khaksari M, Vaezi G, Hojati V, Shiravi A. Hydrogen sulfide protects hippocampal neurons against methamphetamine neurotoxicity via inhibition of apoptosis and neuroinflammation. *J Mol Neurosci*. 2019;67(1):133–141. https://doi.org/10.1007/s12031-018-1218-8.
76. Kimura H. Signaling by hydrogen sulfide (H_2S) and polysulfides (H_2Sn) in the central nervous system. *Neurochem Int*. 2019;126:118–125. https://doi.org/10.1016/j.neuint.2019.01.027.
77. Ha CZ. *Study on the Role of Hydrogen Sulfide in the Pathogenesis of Osteoarthritis of the Knee Joint*. PhD Thesis. Qingdao University; 2016.
78. Leng MH, Mao HM, Shu L. Study on the therapeutic effect of dopamine on osteoarthritis and related molecular mechanism. *Chin J Tradit Med Traumatol Orthop*. 2020;28(9):16–22.
79. Shi R, Gao SS, Zhang J, et al. Collagen prolyl 4-hydroxylases modify tumor progression. *Acta Biochim Biophys Sin*. 2021;53(7):805–814. https://doi.org/10.1093/abbs/gmab065.